École Doctorale des Sciences de l'Environnement d'Île-de-France

Année Universitaire 2018-2019

Modélisation Numérique de l'Écoulement Atmosphérique et Assimilation de Données

Olivier Talagrand

Cours 2

21 Février 2019

- Compléments et précisions sur la circulation générale de l'atmosphère et la modélisation numérique

- Prévision Météorologique Numérique. Performances (d'après CEPMMT)

- Le système d'observation météorologique

- Assimilation. Les bases de l'estimation statistique

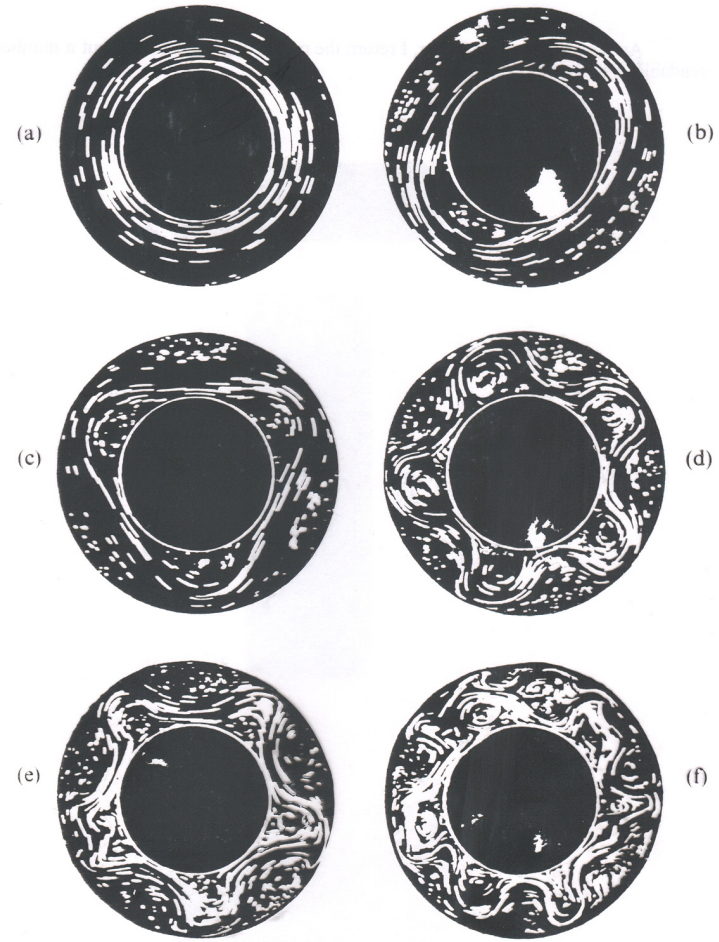

Fig. 10.1. Streak photographs illustrating the dependence of the flow type on rotation rate Ω for a laboratory 'dishpan' experiment. The values of Ω in rad s^{-1} are (a) 0.41; (b) 1.07; (c) 1.21; (d) 3.22; (e) 3.91; (f) 6.4. Working fluid was a water–glycerol solution of mean density 1.037 g cm^{-3} and kinematic viscosity 1.56×10^{-2} cm^2 s^{-1}. The streak photographs show the flow at a depth of 0.5 cm below the free upper surface (see also problem 10.1.) (From Hide & Mason, 1975)

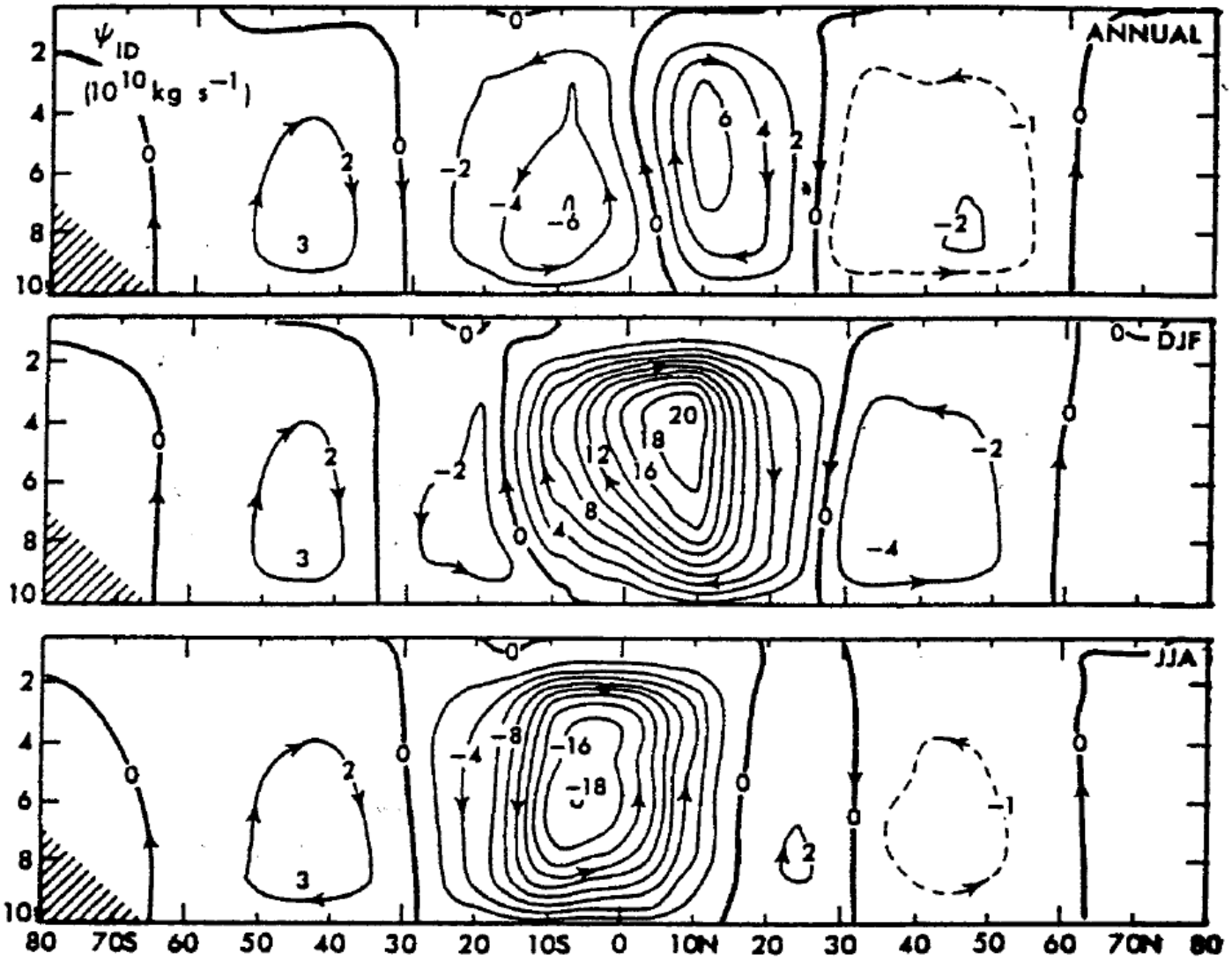

Peixoto and Oort, 1992, *The Physics of Climate,* Springer-Verlag

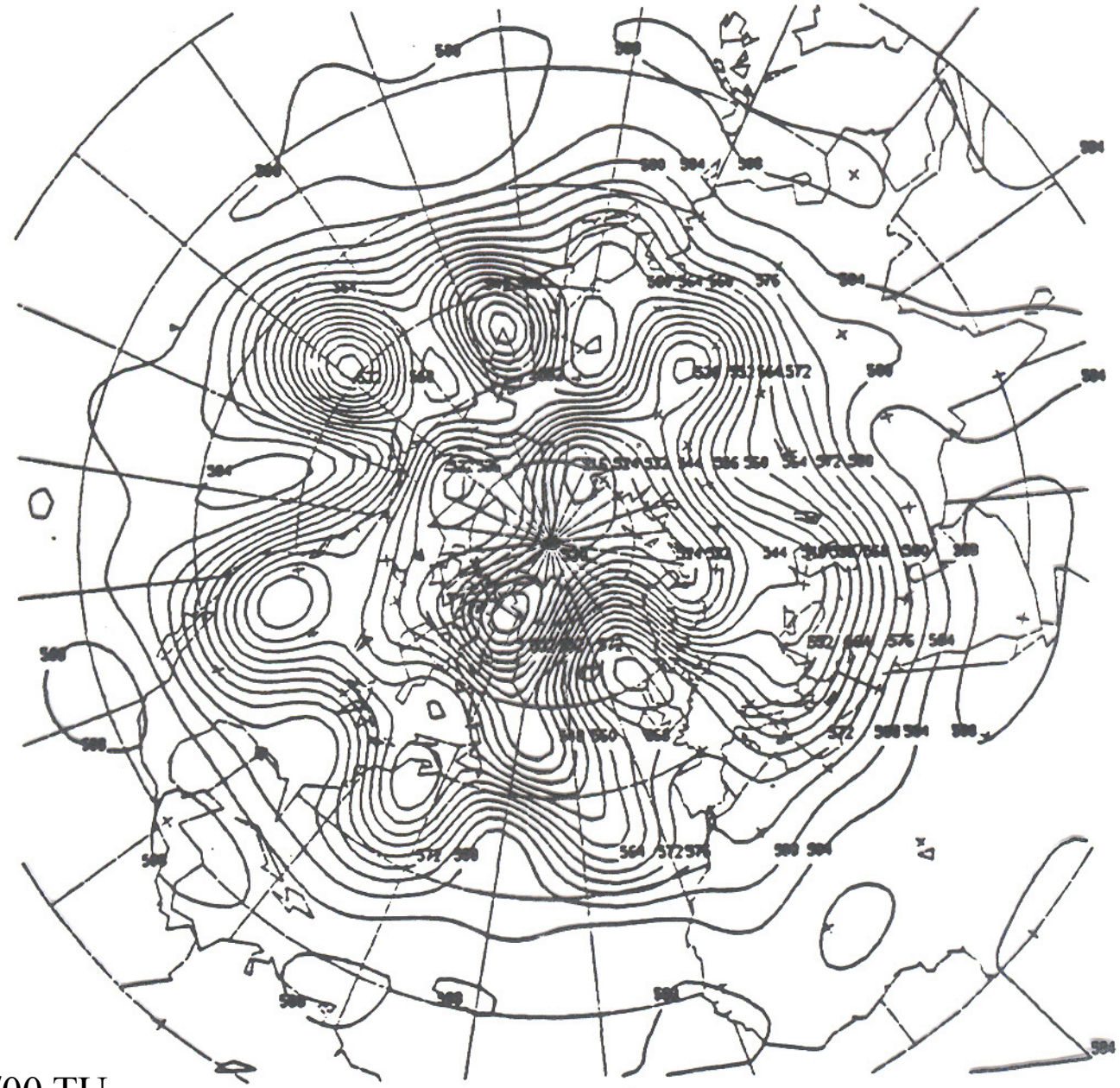

26/04/1984, 00/00 TU

Physical laws governing the flow

- Conservation of mass

  $D\rho/Dt + \rho\,\mathrm{div}\underline{U} = 0$

- Conservation of energy

  $De/Dt - (p/\rho^2)\, D\rho/Dt = Q$

- Conservation of momentum

  $D\underline{U}/Dt + (1/\rho)\,\mathrm{grad}p - \underline{g} + 2\,\underline{\Omega} \wedge \underline{U} = \underline{F}$

- Equation of state

  $f(p, \rho, e) = 0$ $\qquad\qquad$ $(p/\rho = rT,\ e = C_v T)$

- Conservation of mass of secondary components (water in the atmosphere, salt in the ocean, chemical species, …)

  $Dq/Dt + q\,\mathrm{div}\underline{U} = S$

These physical laws must be expressed in practice in discretized (and necessarily imperfect) form, both in space and time

Temporal discretization. Courant-Friedrichs-Lewy (CFL) condition for stability of explicit schemes

$$\Delta t / \Delta x < \alpha / c$$

where c is phase velocity of fastest propagating (wave) in the system, and α is an $O(1)$ numerical coefficient depending on particular scheme under consideration.

Significance : numerical propagation of signal must be at least as fast as physical propagation.

In hydrostatic atmosphere, fastest propagating wave : gravity wave with largest scale height, $c = \sqrt{(rT)} \approx 300$ $m.s^{-1}$.

$$\Delta x = 30 \text{ km} \quad \Rightarrow \Delta t = 100 \text{ s}$$

The use of *semi-implicit* schemes allows to get rid of the CFL condition, and to use longer timesteps.

In the parlance of the trade, one distinguishes two different parts in models. The ‘dynamics’ deals with the physically reversible processes (pressure forces, Coriolis force, advection, …), while the ‘physics’ deals with physically irreversible processes, in particular the diabatic heating term Q in the energy equation, and also the parameterization of subgrid scales effects.

Numerical schemes have been gradually developed and validated for the ‘dynamics’ component of models, which are by and large considered now to work satisfactorily (although regular improvements are still being made; project *DYNAMICO*, *Dynamical Core on Icosahedral Grid*, Th. Dubos, IPSL).

The situation is different as concerns ‘physics’, where many problems remain (as concerns for instance subgrid scales parameterization, the water cycle and the associated exchanges of energy, or the exchanges that take place in the boundary layer between the atmosphere and the underlying medium). ‘Physics’ as a whole remains the weaker point of models, and is still the object of active research.

5 - SCHEMA DES INTERACTIONS PHYSIQUES DANS LE MODELE

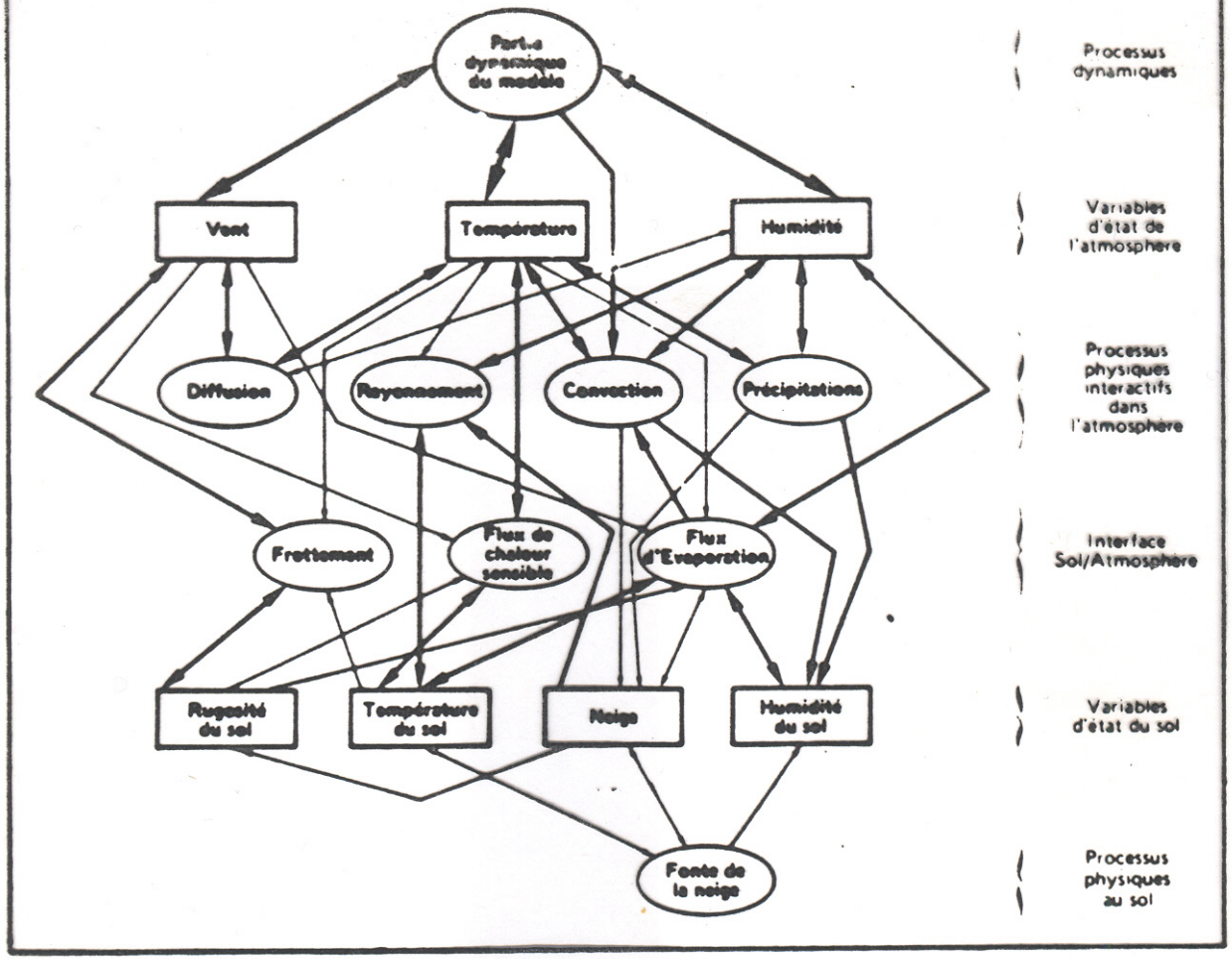

Centre Européen pour les Prévisions Météorologiques à Moyen Terme (CEPMMT, Reading, GB)

(European Centre for Medium-range Weather Forecasts, ECMWF)

Depuis mars 2016 :

Troncature triangulaire TCO1279 / O1280 (résolution horizontale ≈ 9 kilomètres)

137 niveaux dans la direction verticale (0 - 80 km)

Discrétisation en éléments finis dans la direction verticale

Dimension du vecteur d'état correspondant > 10^9

Pas de discrétisation temporelle (schéma semi-Lagrangien semi-implicite): 450 secondes

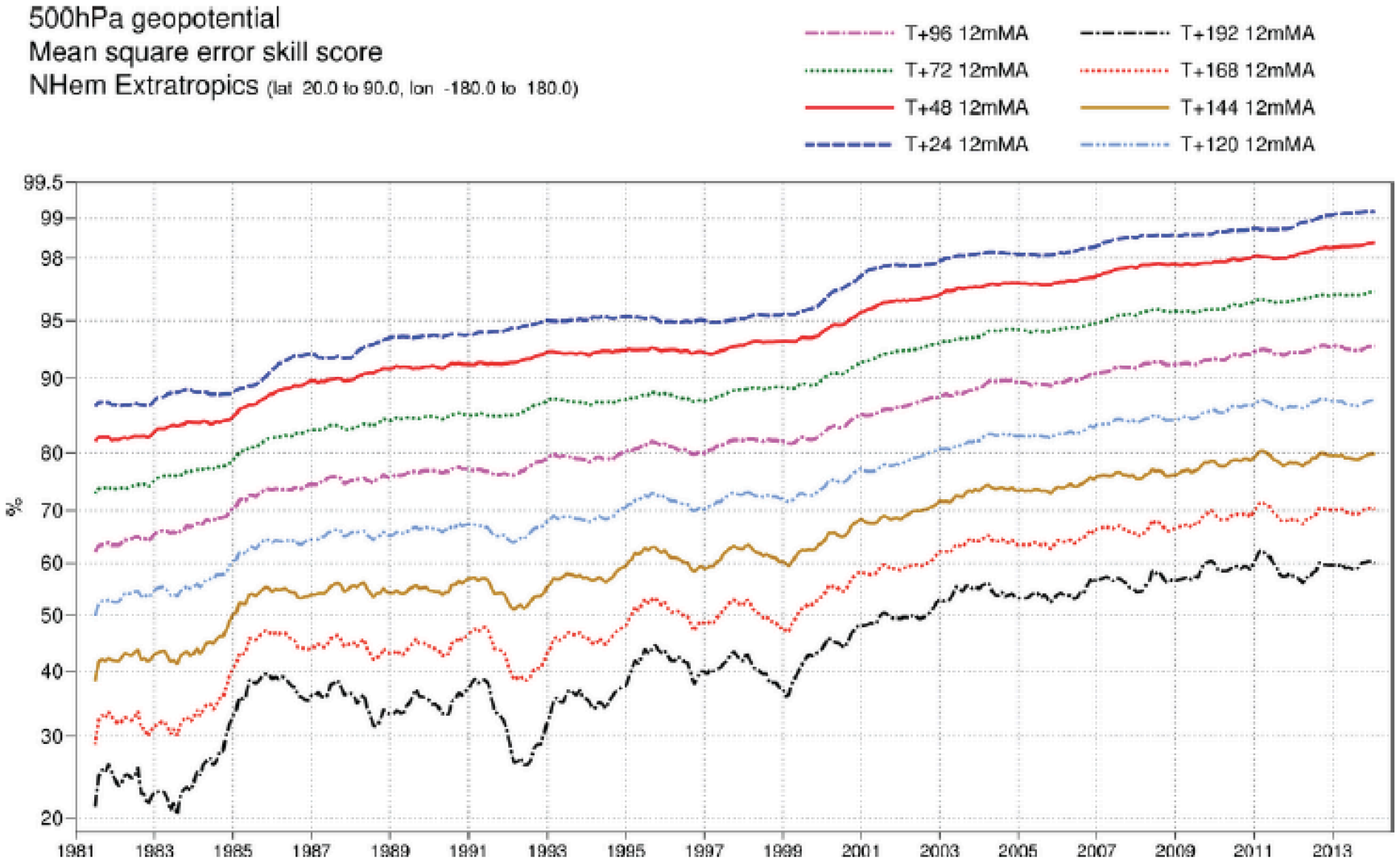

Figure 3: 500 hPa geopotential height mean square error skill score for Europe (top) and the northern hemisphere extratropics (bottom), showing 12-month moving averages for forecast ranges from 24 to 192 hours. The last point on each curve is for the 12-month period August 2013–July 2014.

Persistence = 0 ; climatology = 50 at long range

Results extracted from :

Haiden *et al.*, 2018, *Evaluation of ECMWF forecasts, including the 2018 upgrade*, Technical Memorandum 831, ECMWF, Reading, UK.

Available at the address :

https://www.ecmwf.int/en/elibrary/18746-evaluation-ecmwf-forecasts-including-2018-upgrade

(see also site of ECMWF)

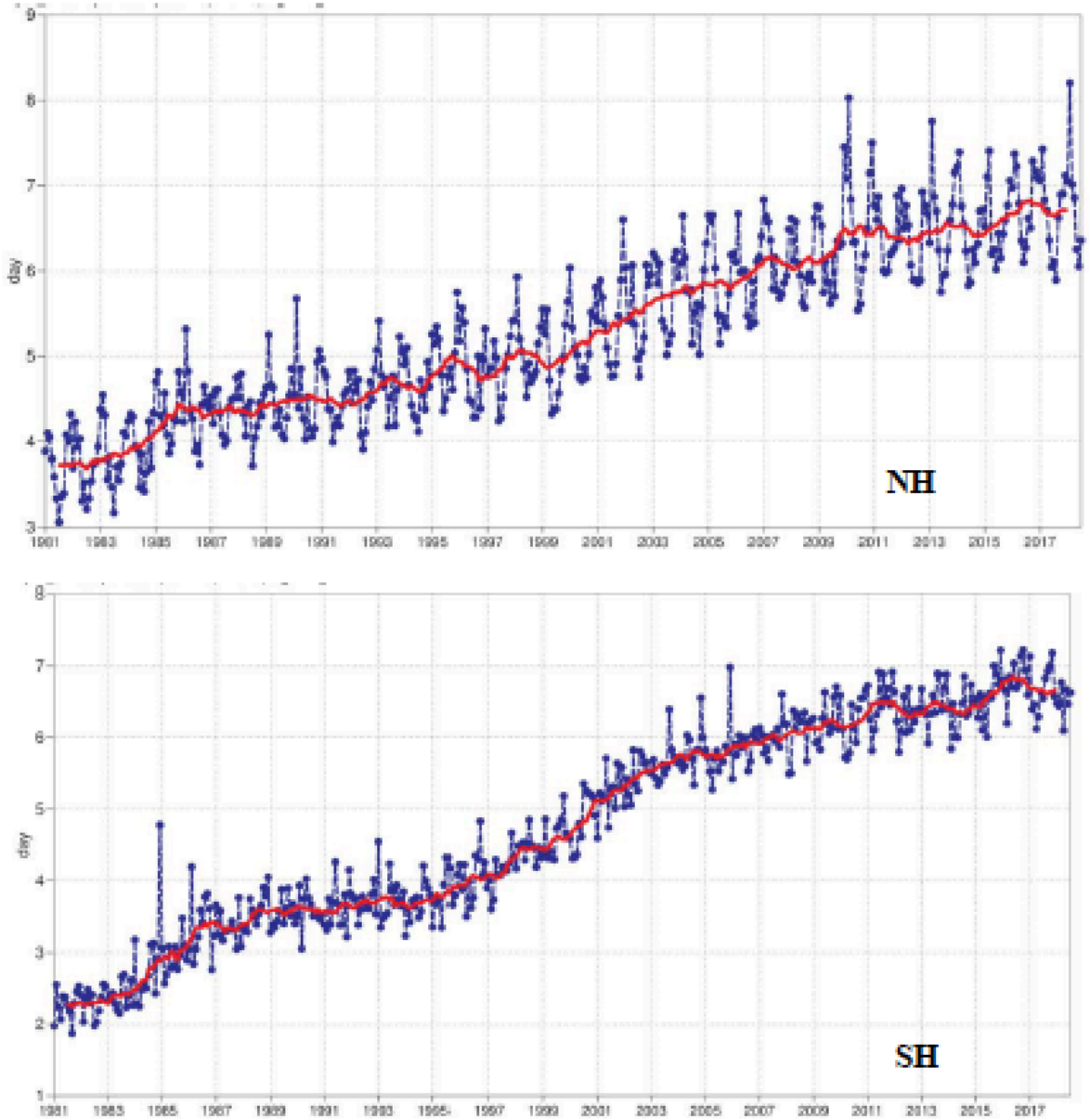

Figure 4: Primary headline score for the high-resolution forecasts. Evolution with time of the 500 hPa geopotential height forecast performance – each point on the curves is the forecast range at which the monthly mean (blue lines) or 12-month mean centred on that month (red line) of the forecast anomaly correlation (ACC) with the verifying analysis falls below 80% for Europe (top), northern hemisphere extratropics (centre) and southern hemisphere extratropics (bottom).

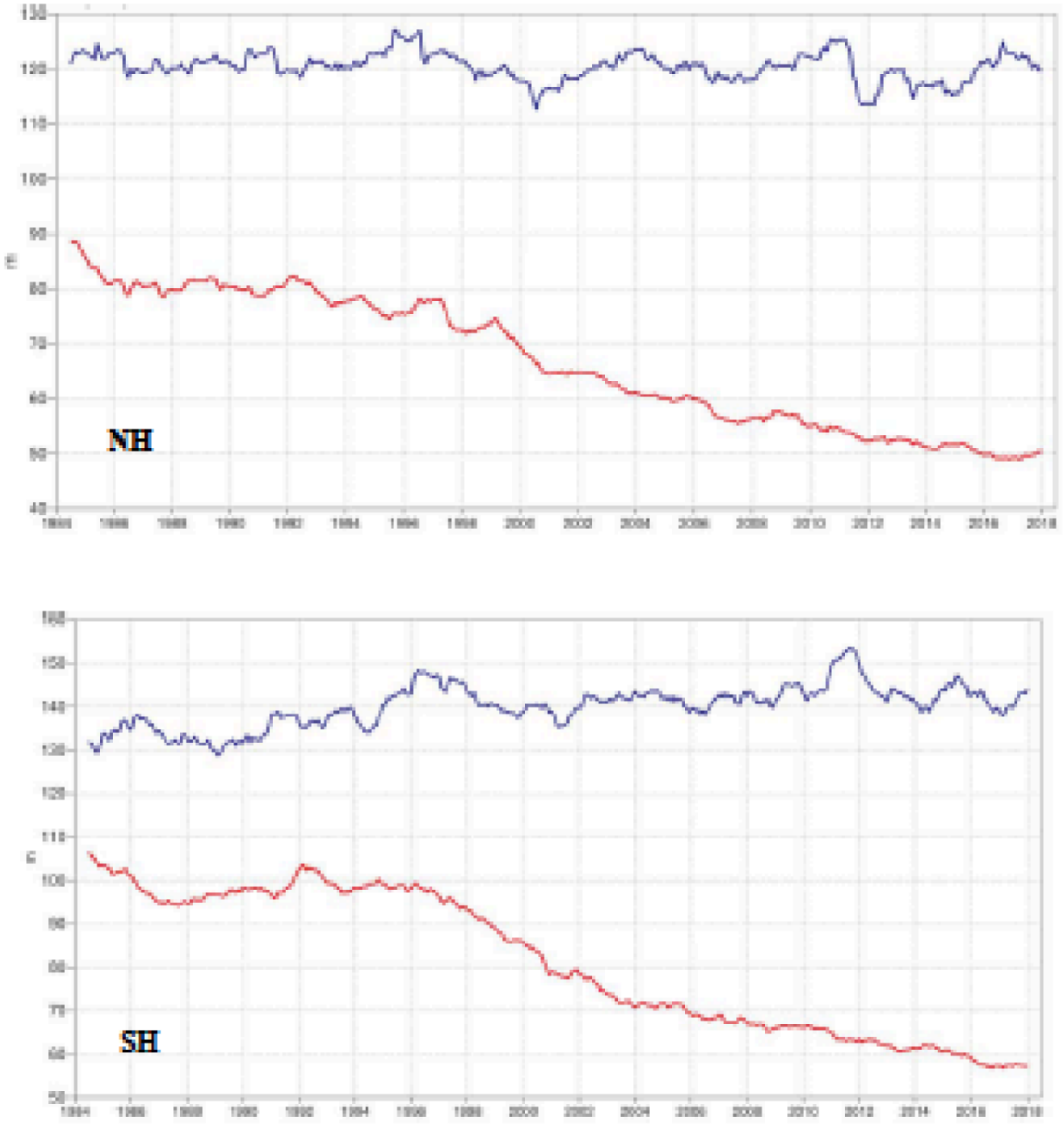

Figure 5: Root mean square (RMS) error of forecasts of 500 hPa geopotential height (m) at day 6 (red), verified against analysis. For comparison, a reference forecast made by persisting the analysis over 6 days is shown (blue). Plotted values are 12-month moving averages; the last point on the curves is for the 12-month period August 2017–July 2018. Results are shown for the northern extra-tropics (top), and the southern extra-tropics (bottom).

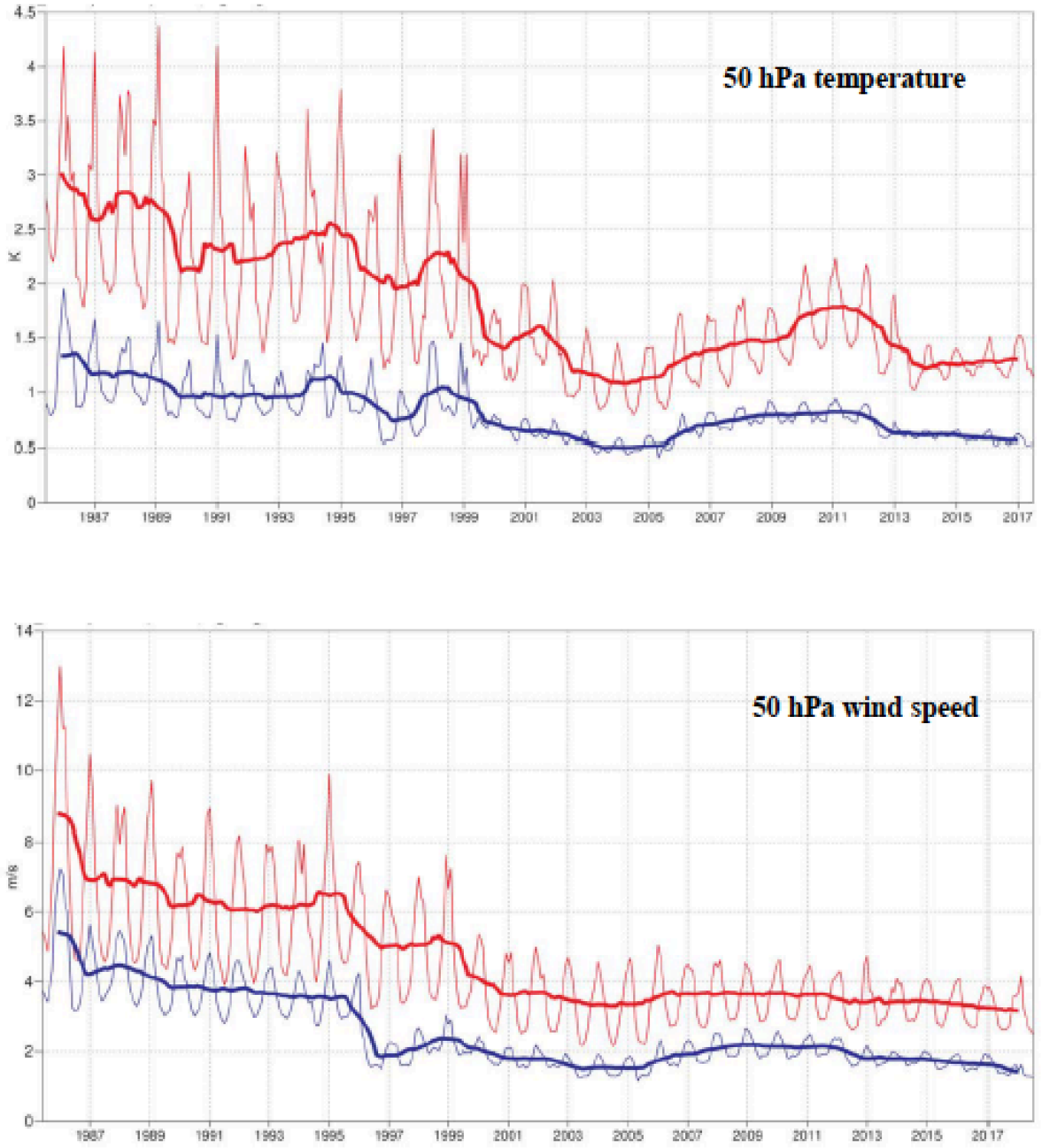

Figure 7: Model scores for temperature (top) and wind (bottom) in the northern extratropical stratosphere. Curves show the monthly average RMS temperature and vector wind error at 50 hPa for one-day (blue) and five-day (red) forecasts, verified against analysis. 12-month moving average scores are also shown (in bold).

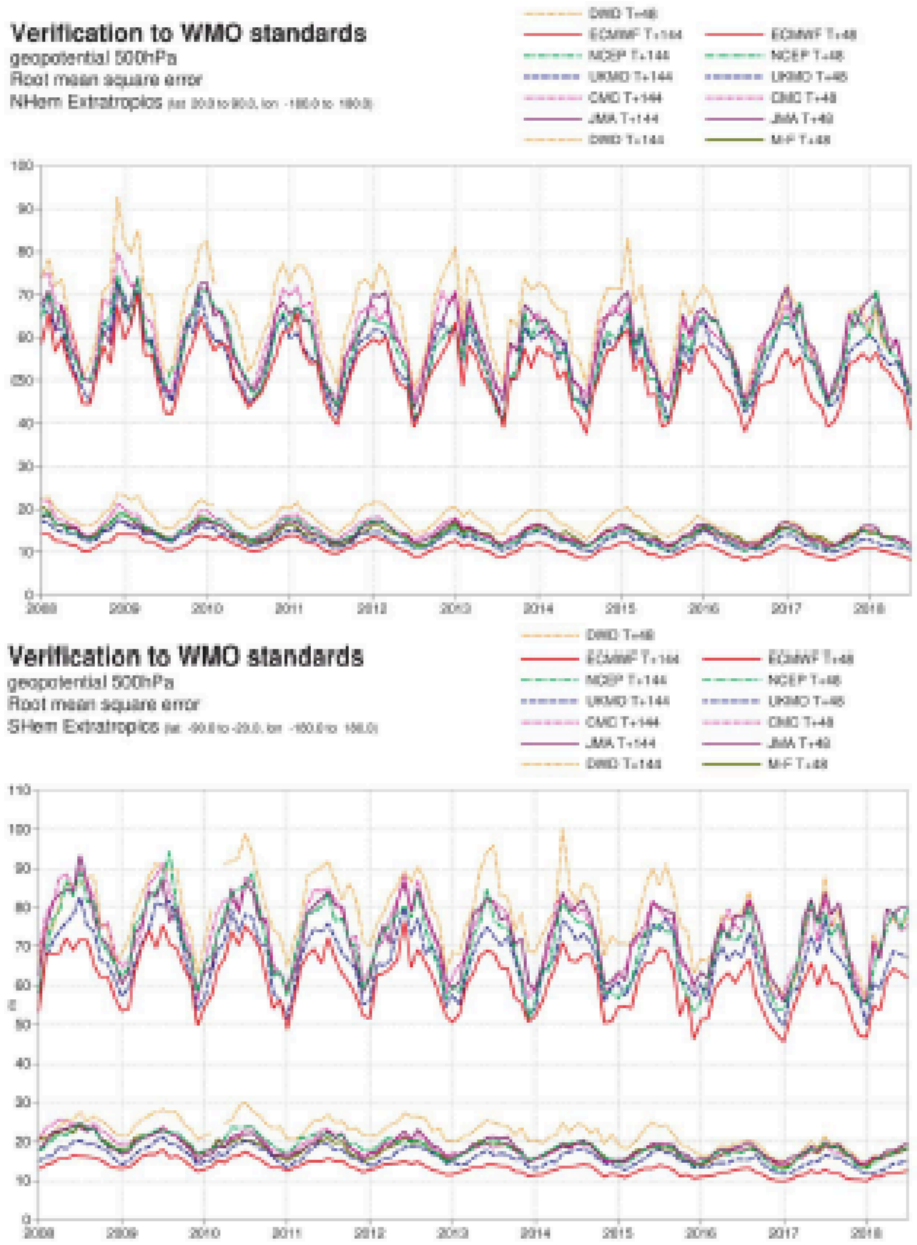

Figure 14: WMO-exchanged scores from global forecast centres. RMS error of 500 hPa geopotential height over northern (top) and southern (bottom) extratropics. In each panel, the upper curves show the six-day forecast error and the lower curves show the two-day forecast error of model runs initiated at 12 UTC. Each model is verified against its own analysis. JMA = Japan Meteorological Agency, CMC = Canadian Meteorological Centre, UKMO = the UK Met Office, NCEP = U.S. National Centers for Environmental Prediction, M-F = Météo France, DWD = Deutscher Wetterdienst.

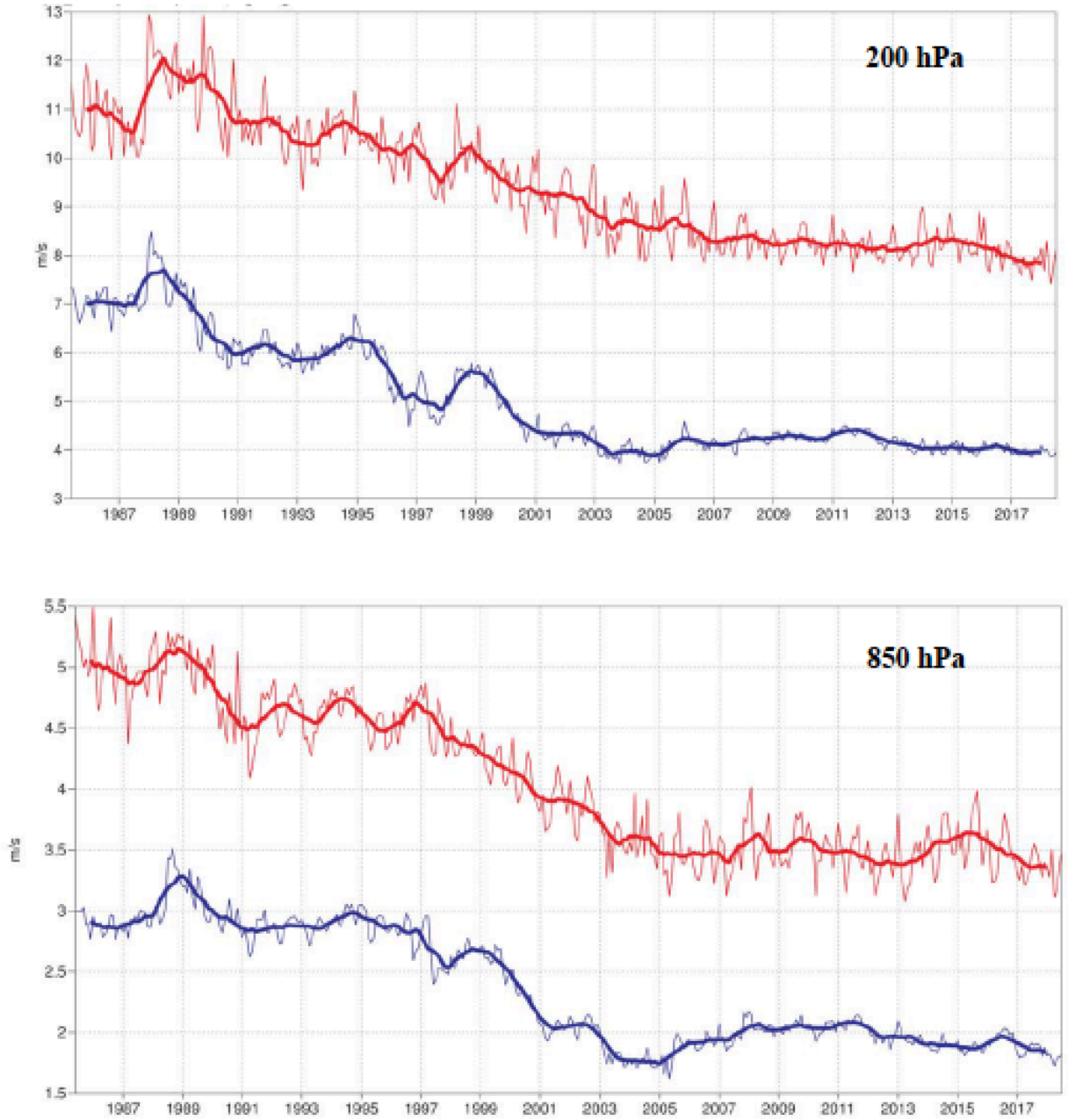

Figure 13: Forecast performance in the tropics. Curves show the monthly average RMS vector wind errors at 200 hPa (top) and 850 hPa (bottom) for one-day (blue) and five-day (red) forecasts, verified against analysis. 12-month moving average scores are also shown (in bold).

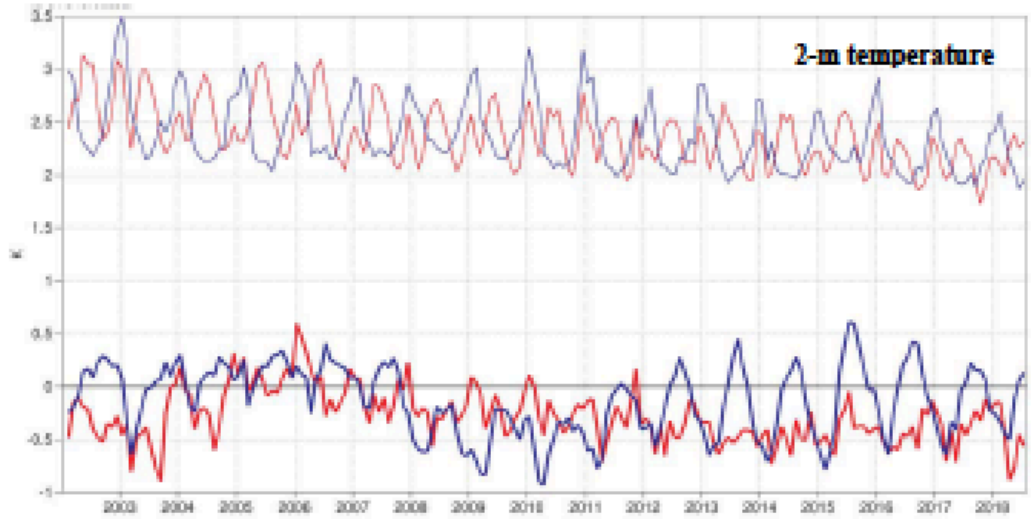

Figure 21: Verification of 2 m temperature forecasts against European SYNOP data on the GTS for 60-hour (night-time) and 72-hour (daytime) forecasts. Lower pair of curves shows bias, upper curves are standard deviation of error.

Night time: blue curves
Day time: red curves

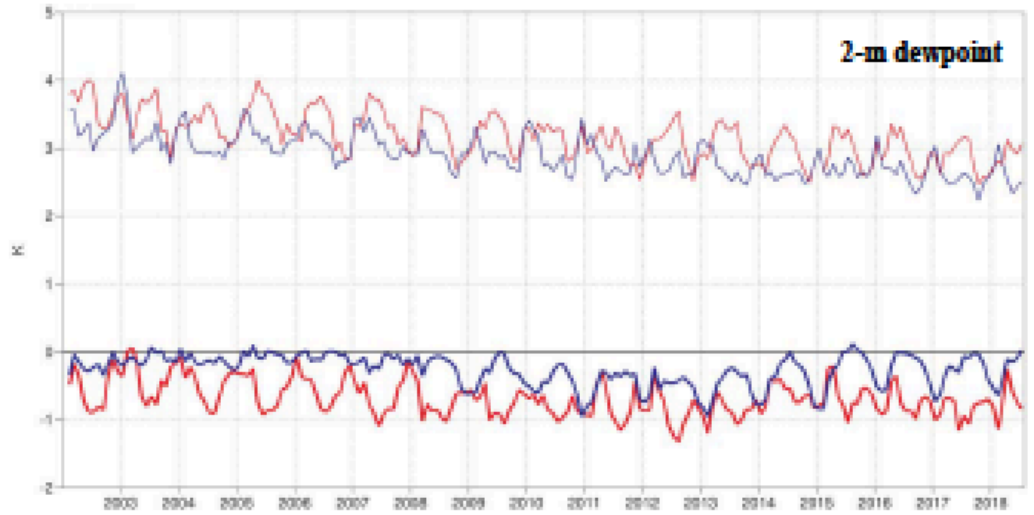

Figure 22: Verification of 2 m dew point forecasts against European SYNOP data on the Global Telecommunication System (GTS) for 60-hour (night-time) and 72-hour (daytime) forecasts. Lower pair of curves shows bias, upper curves show standard deviation of error.

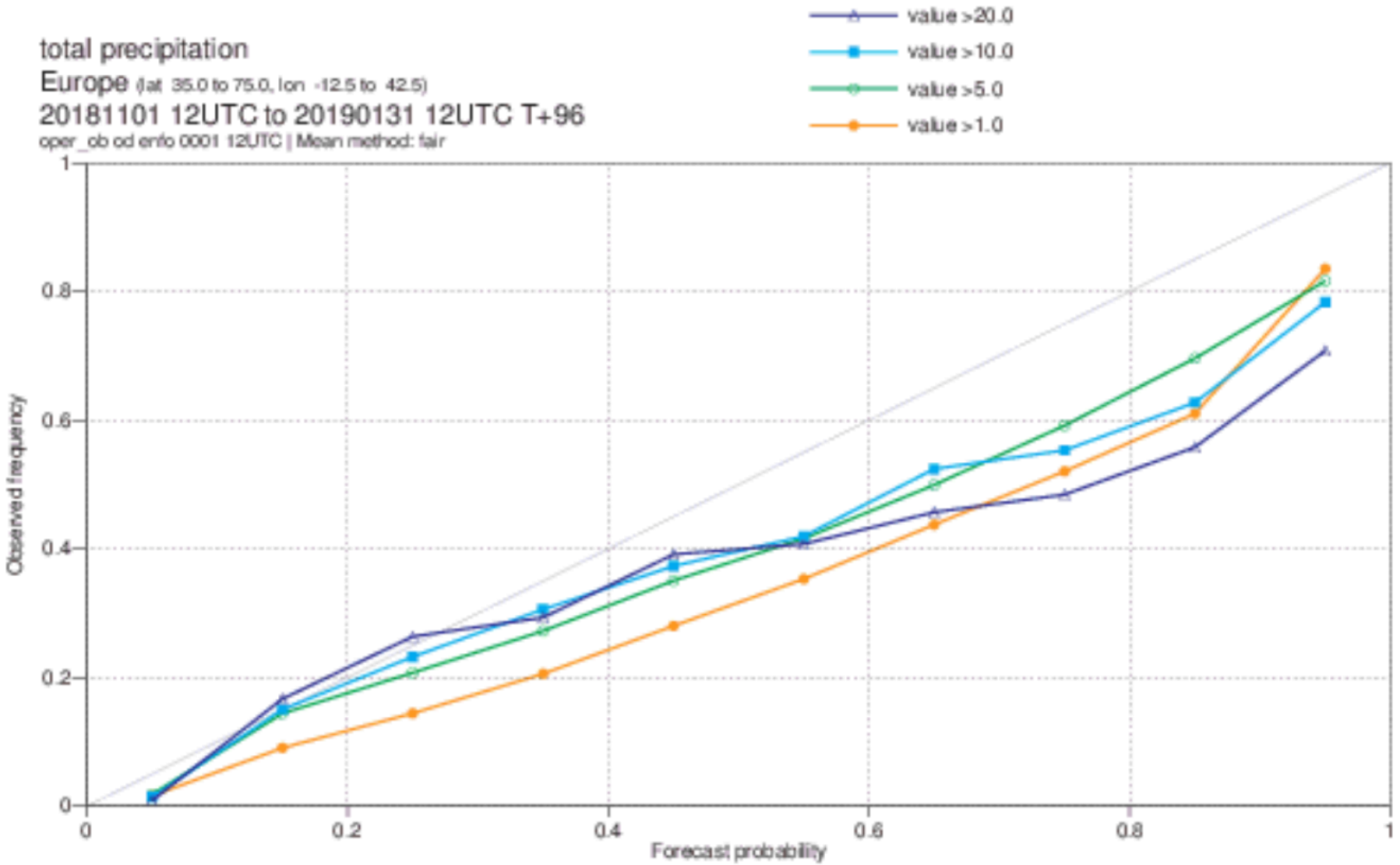
total precipitation
Europe (lat 35.0 to 75.0, lon -12.5 to 42.5)
20181101 12UTC to 20190131 12UTC T+96
oper_ob od enfo 0001 12UTC | Mean method: fair
value >20.0
value >10.0
value >5.0
value >1.0
Observed frequency
Forecast probability
0
0.2
0.4
0.6
0.8
1

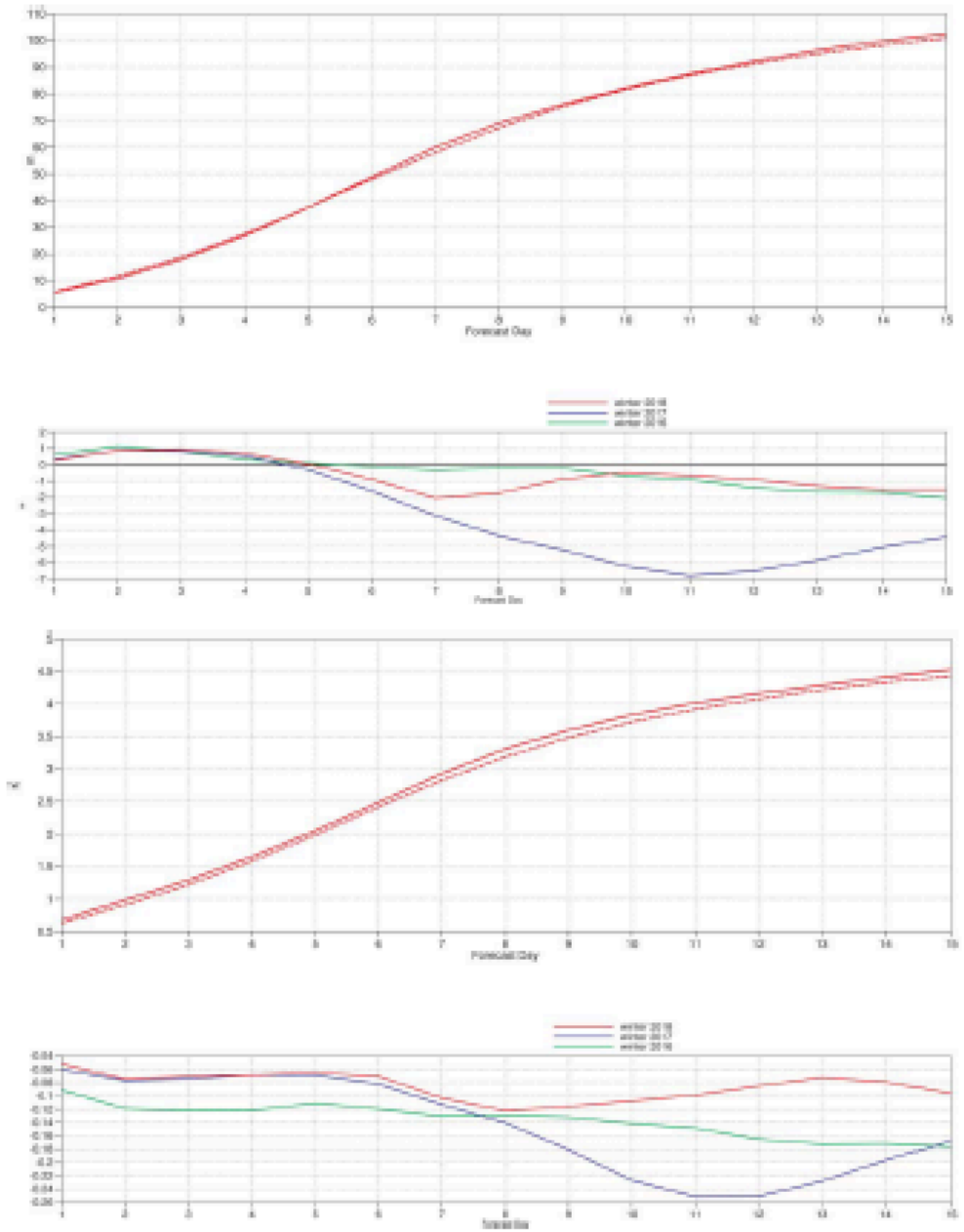

Figure 9: Ensemble spread (standard deviation, dashed lines) and RMS error of ensemble-mean (solid lines) for winter 2017–2018 (upper figure in each panel), and differences of ensemble spread and RMS error of ensemble mean for last three winter seasons (lower figure in each panel, negative values indicate spread is too small); verification is against analysis, plots are for 500 hPa geopotential (top) and 850 hPa temperature (bottom) over the extratropical northern hemisphere for forecast days 1 to 15.

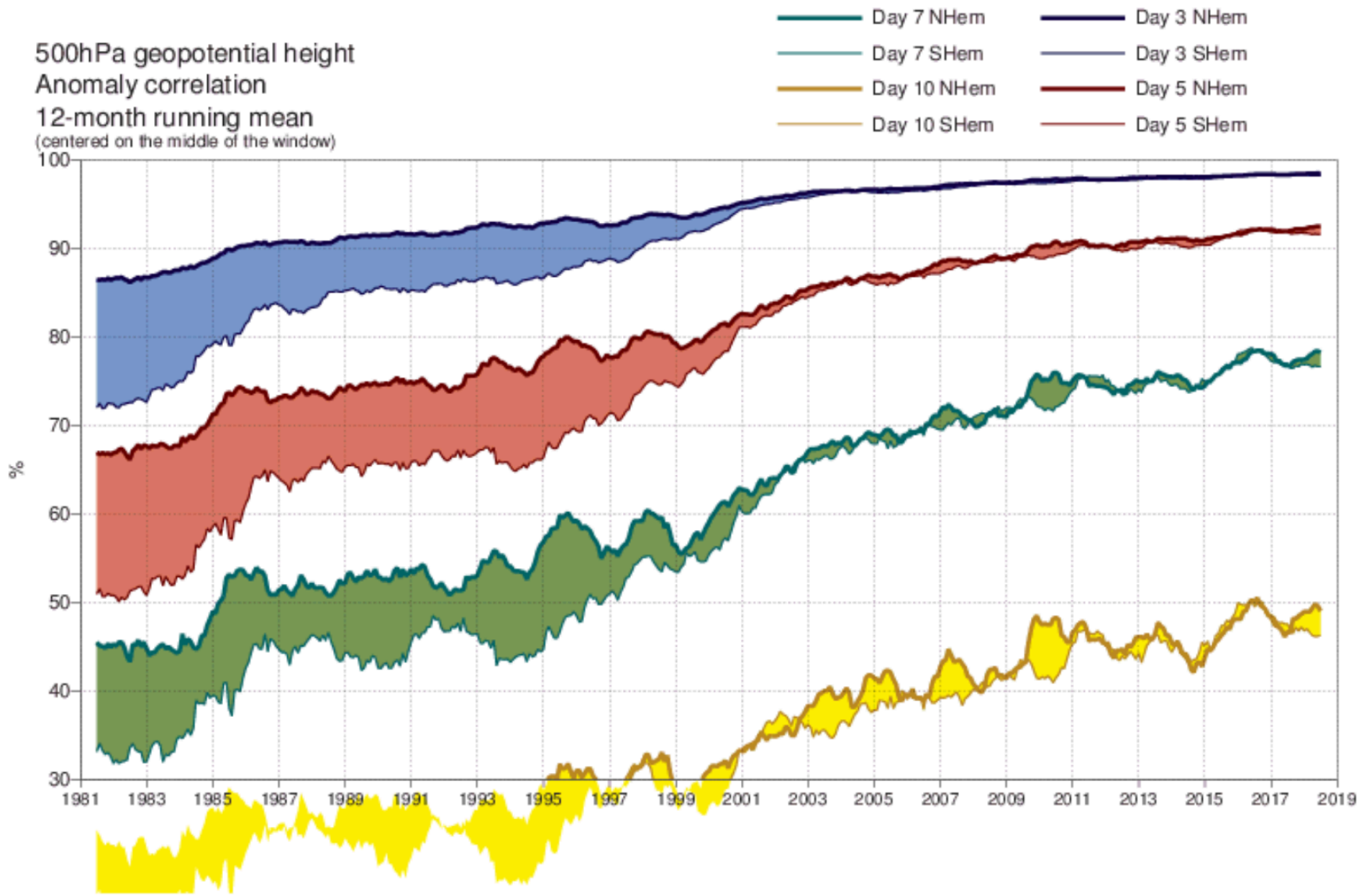

Anomaly correlation of ECMWF 500hPa height forecasts

ECMWF

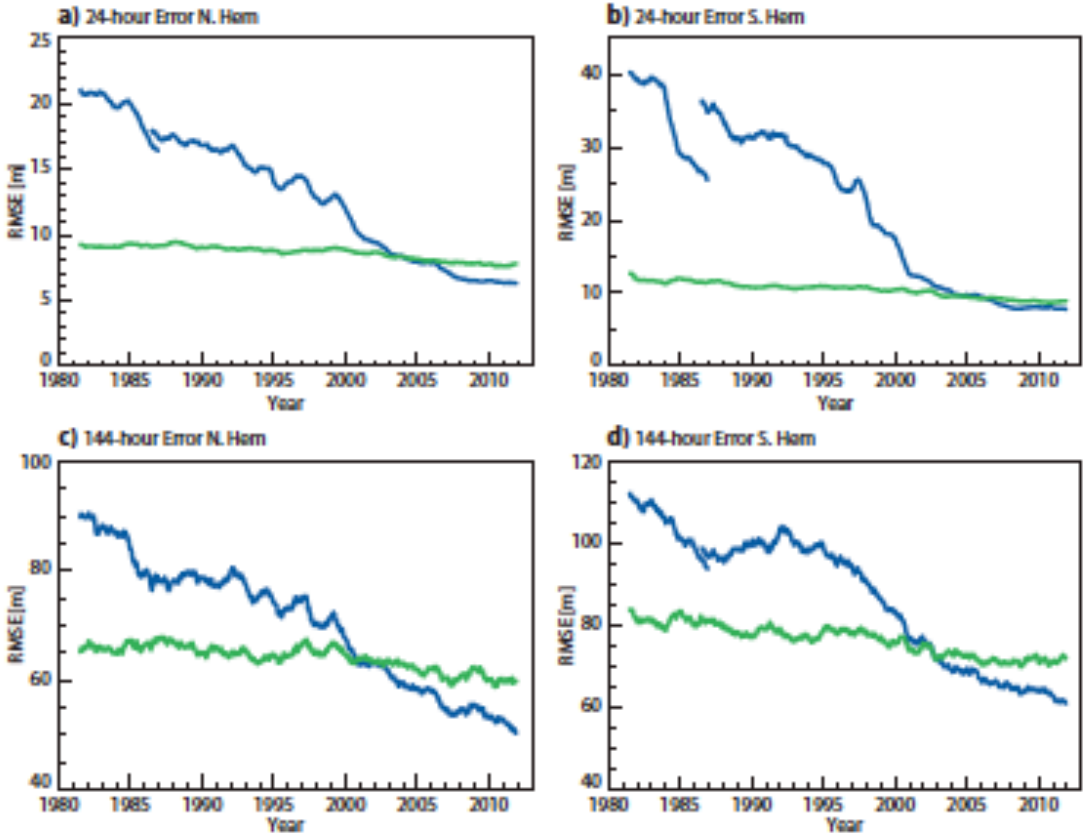

FIG. 3. Evolution of forecast errors from 1981 to 2012 for N.Hem (a and c) and S.Hem (b and d). Operational forecasts (blue) and ERA Interim (green). Note that before 1986 the operational analysis is used to verify the operational forecasts, after 1986 ERA Interim is used for the verification (with an overlap of 6 months present).

Magnusson and Källén, 2013, *Mon. Wea. Rev.*, **141**, 3142–3153

Problèmes restants

- Cycle de l'eau (évaporation, condensation, influence sur le rayonnement absorbé ou émis par l'atmosphère)

- Échanges avec l'océan ou la surface continentale (chaleur, eau, quantité de mouvement, …)

- …

850 hPa temperature / 500 hPa geopotential

Tuesday 19 Feb, 00 UTC T+192 Valid: Wednesday 27 Feb, 00 UTC

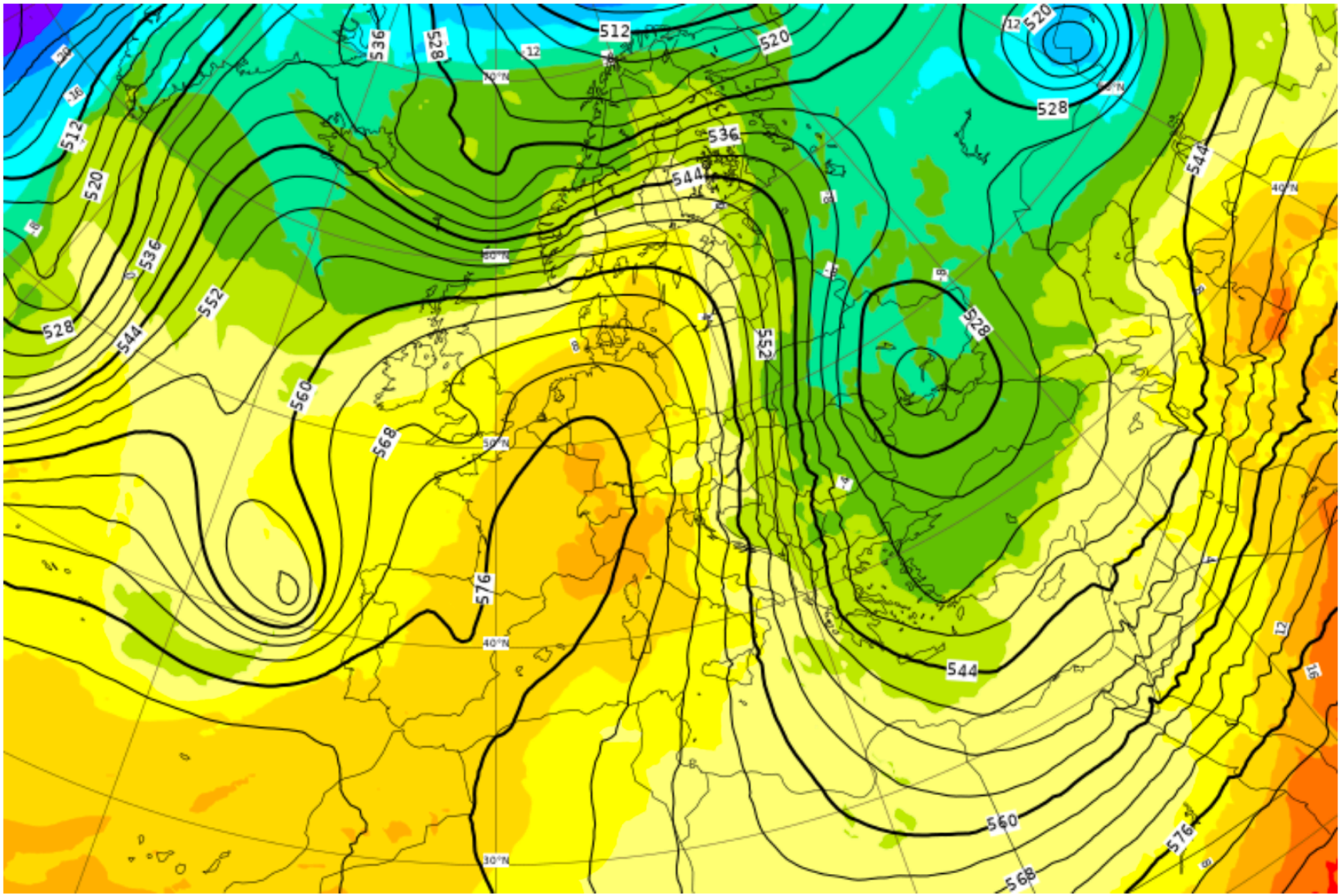

ECMWF data coverage (all observations) - SYNOP-SHIP-METAR

19/02/2019 00

Total number of obs = 104896

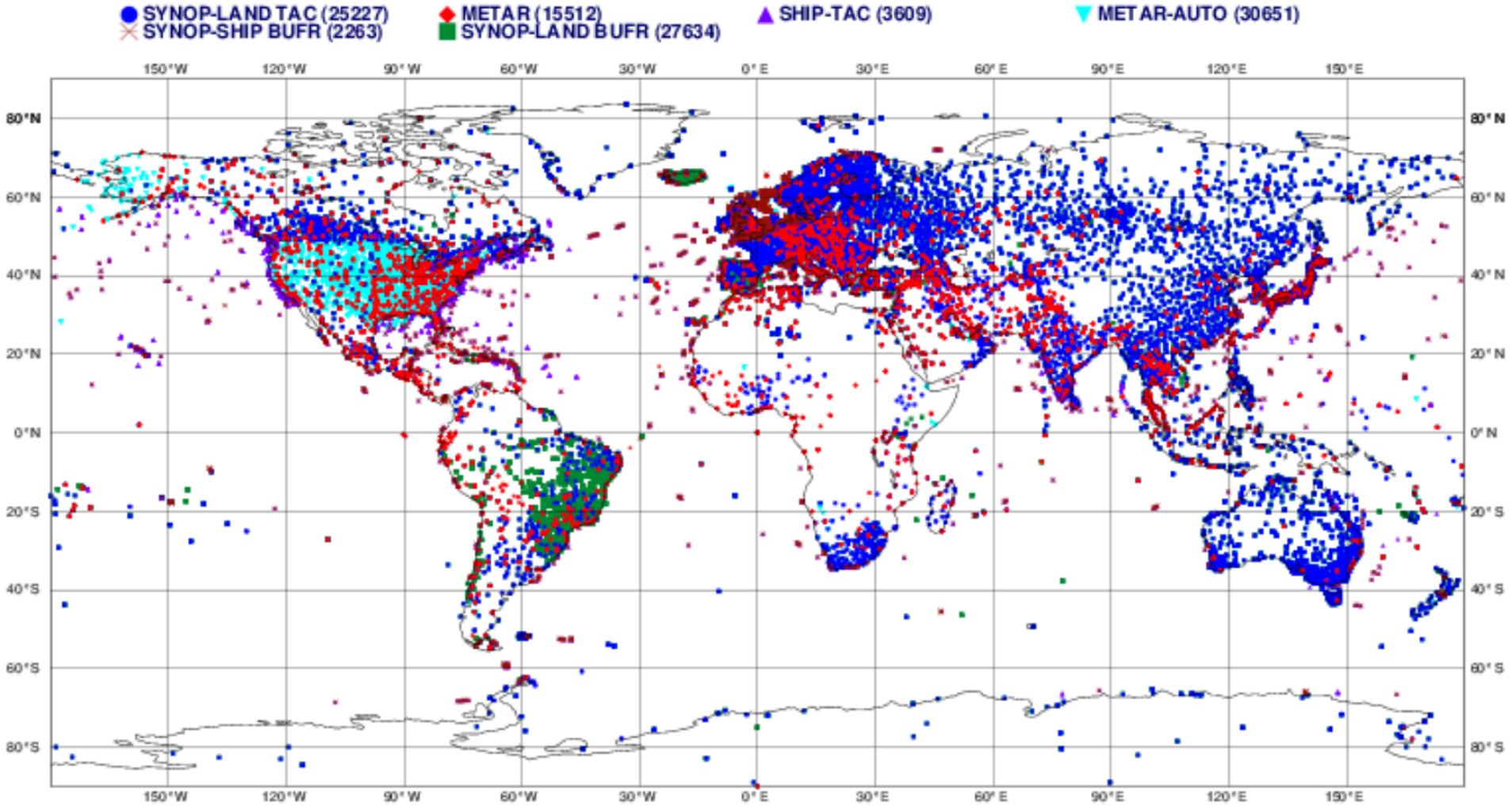

ECMWF data coverage (all observations) - RADIOSONDE

19/02/2019 00

Total number of obs = 3429

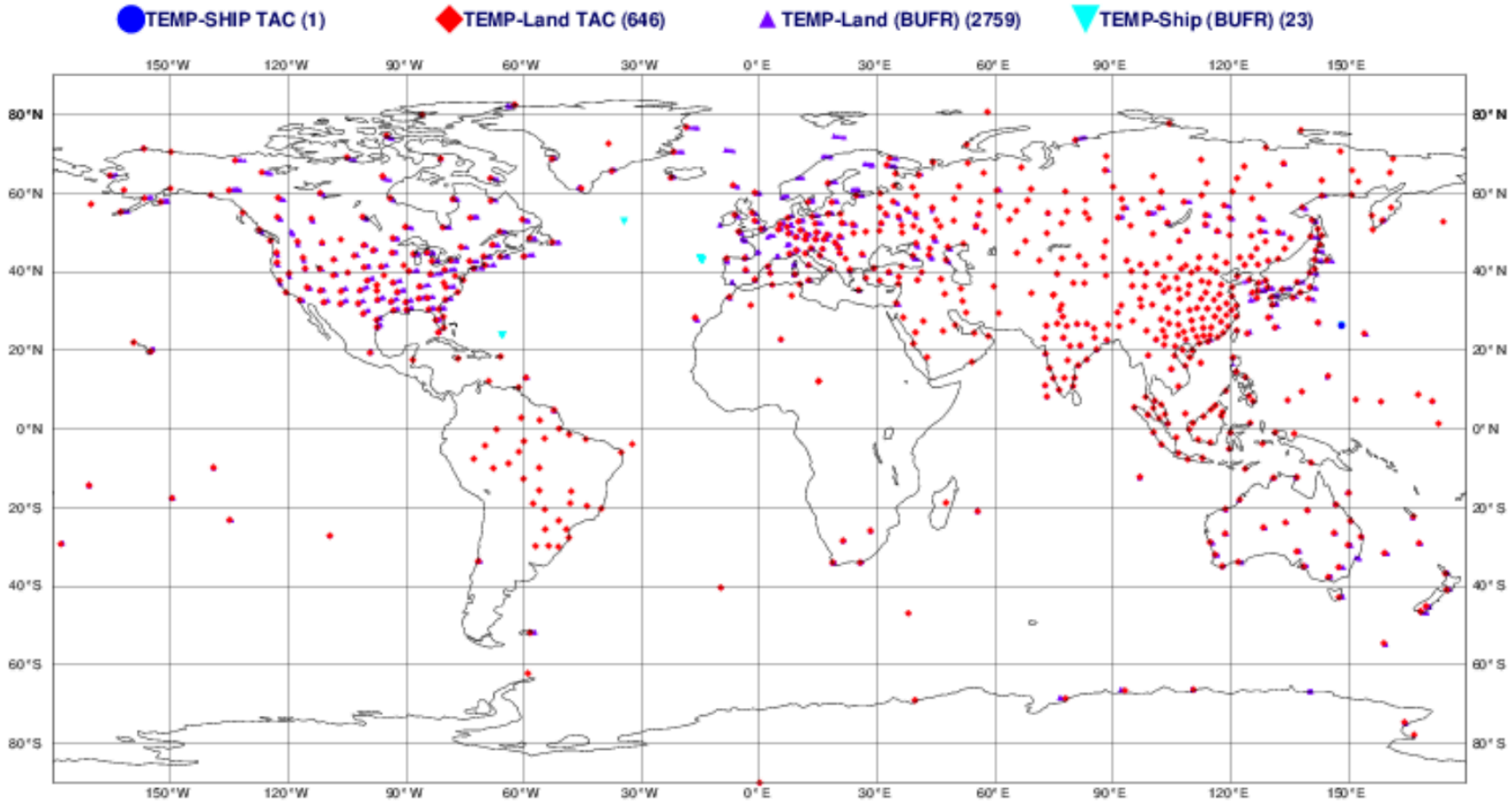

ECMWF data coverage (all observations) - AIRCRAFT
19/02/2019 00
Total number of obs = 235848

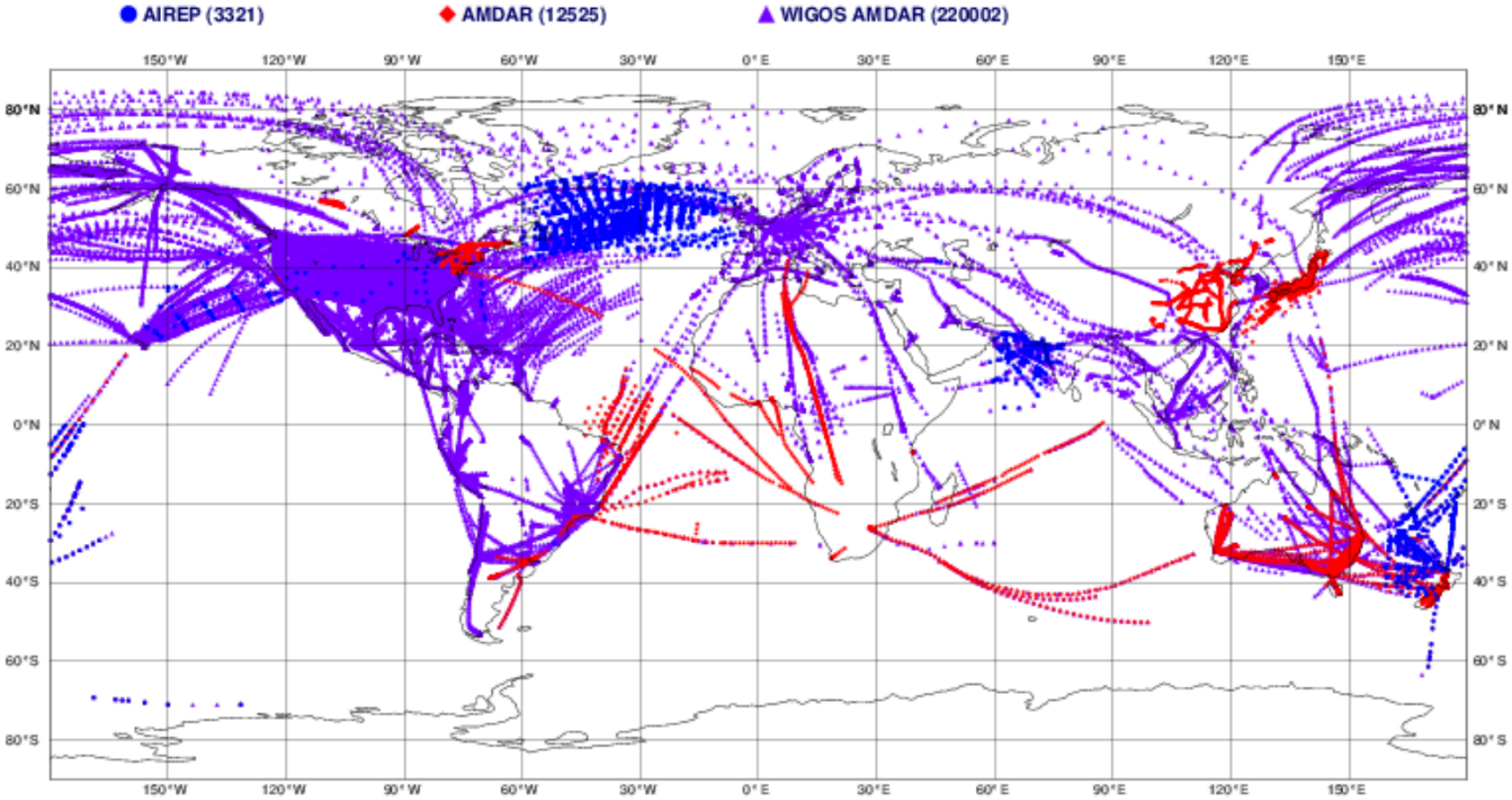

ECMWF data coverage (all observations) - AMSUA

19/02/2019 00

Total number of obs = 597613

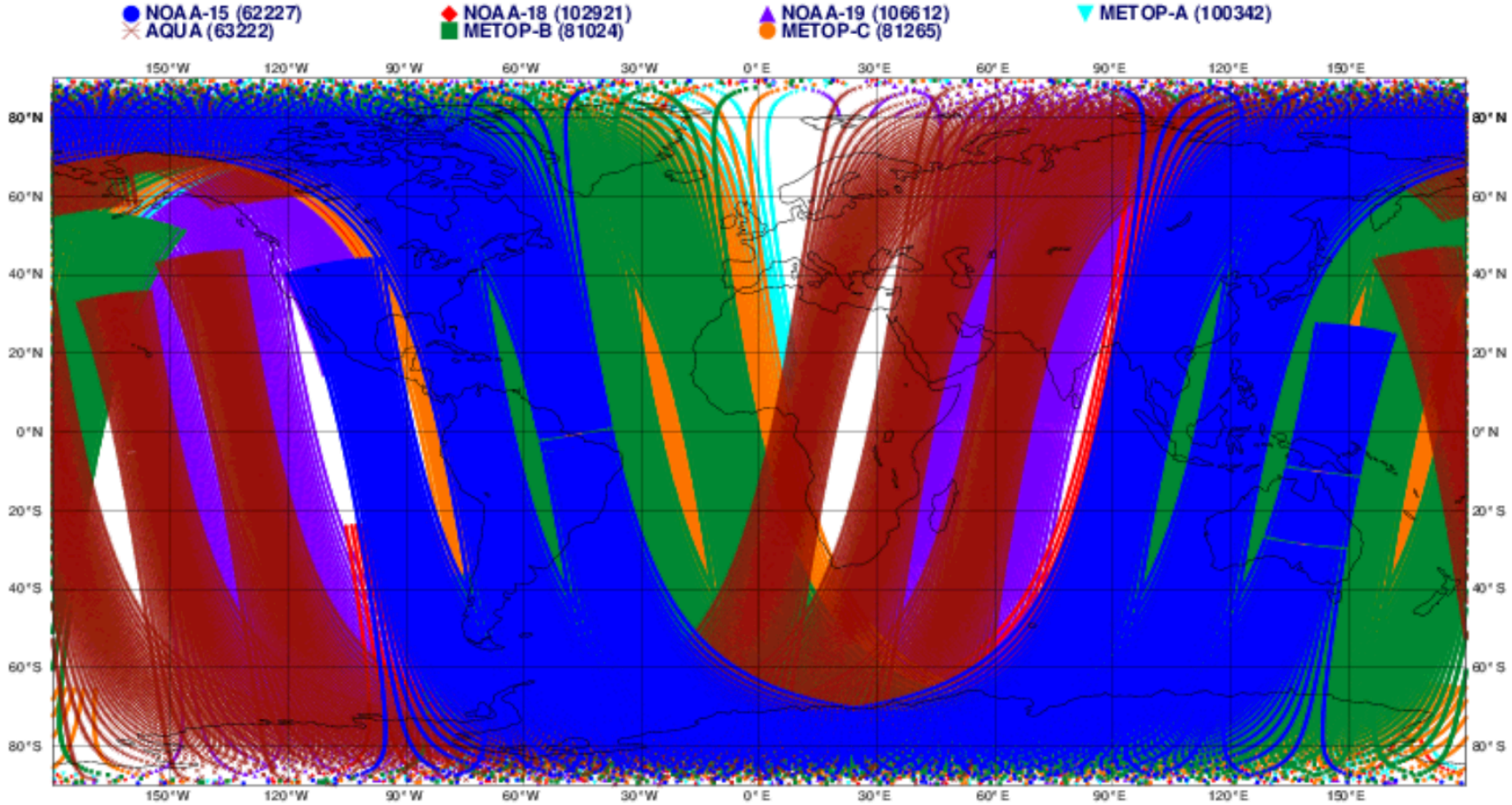

ECMWF data coverage (all observations) - AMV WV

19/02/2019 00

Total number of obs = 674718

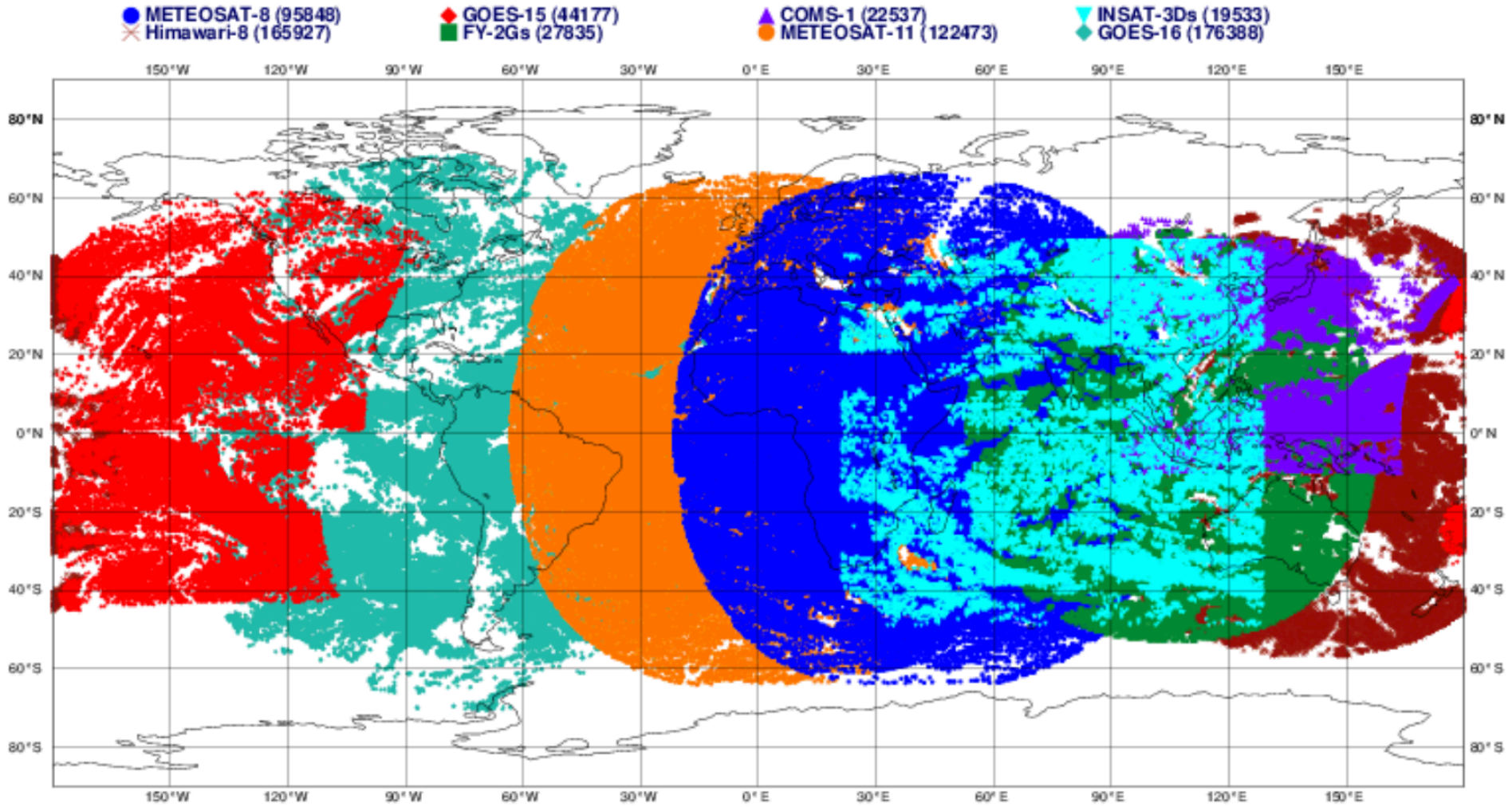

ECMWF data coverage (all observations) - AMV VIS

19/02/2019 00

Total number of obs = 576554

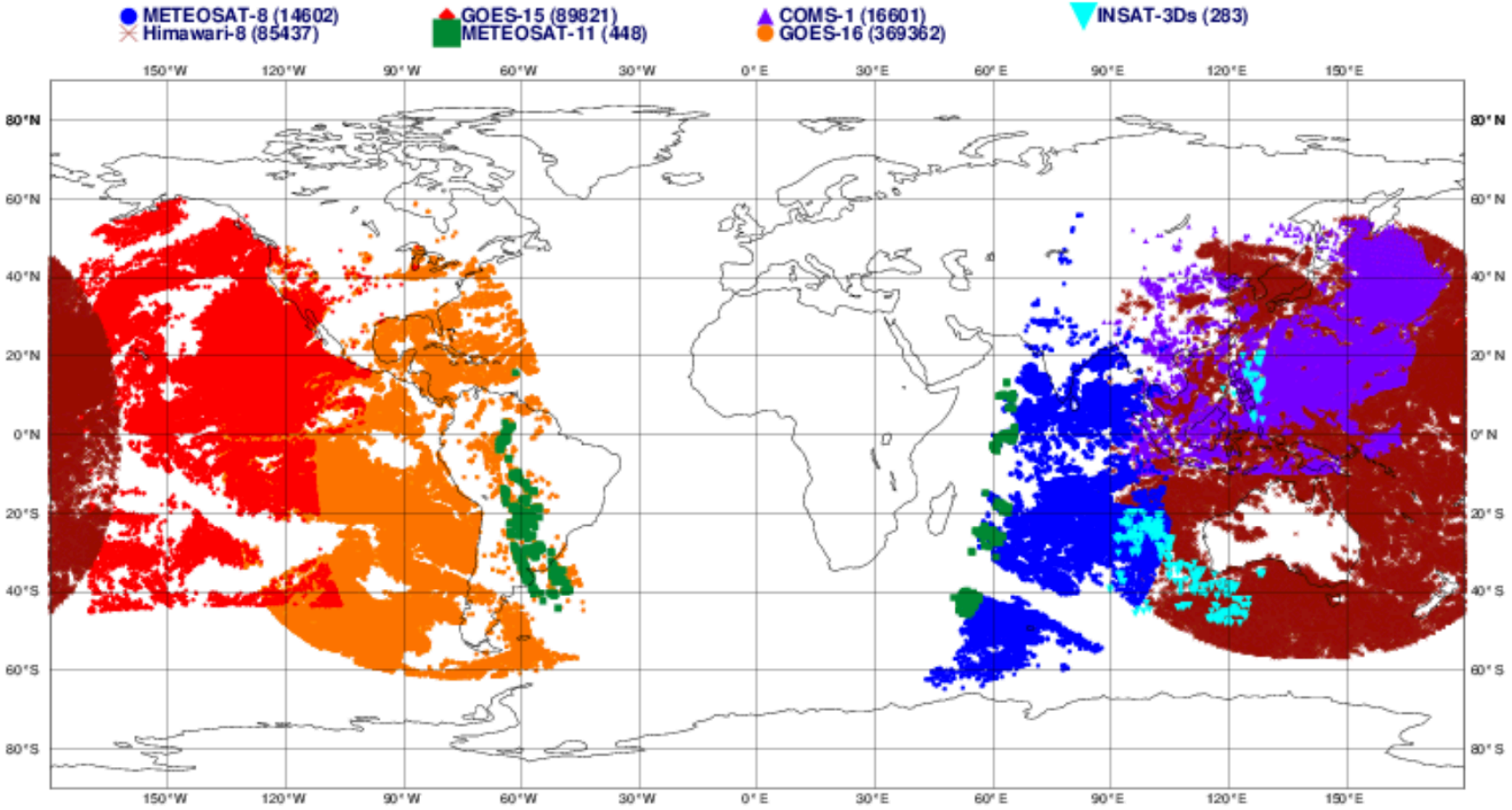

ECMWF data coverage (all observations) - GPSRO

19/02/2019 00

Total number of obs = 17521

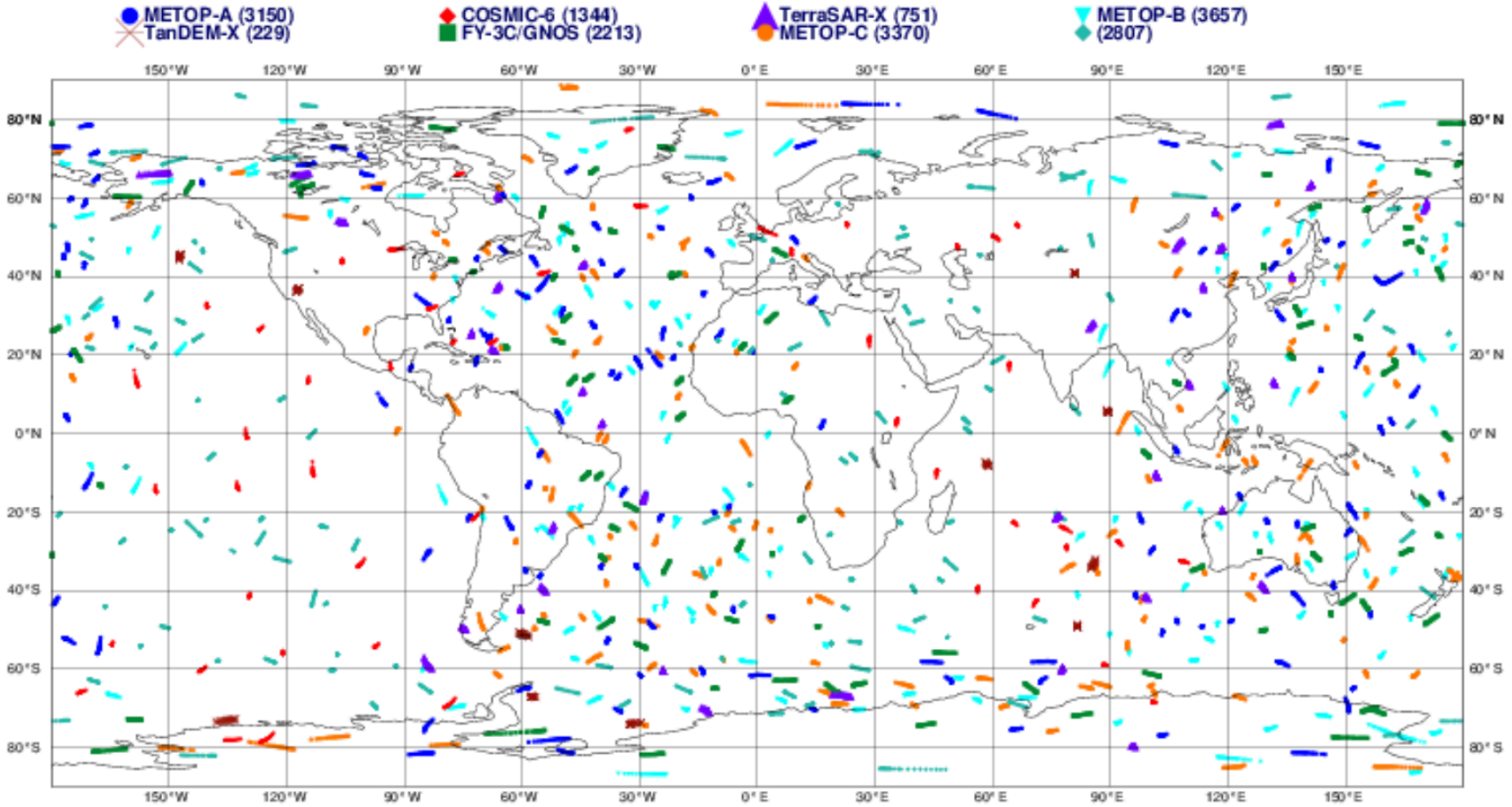

ECMWF

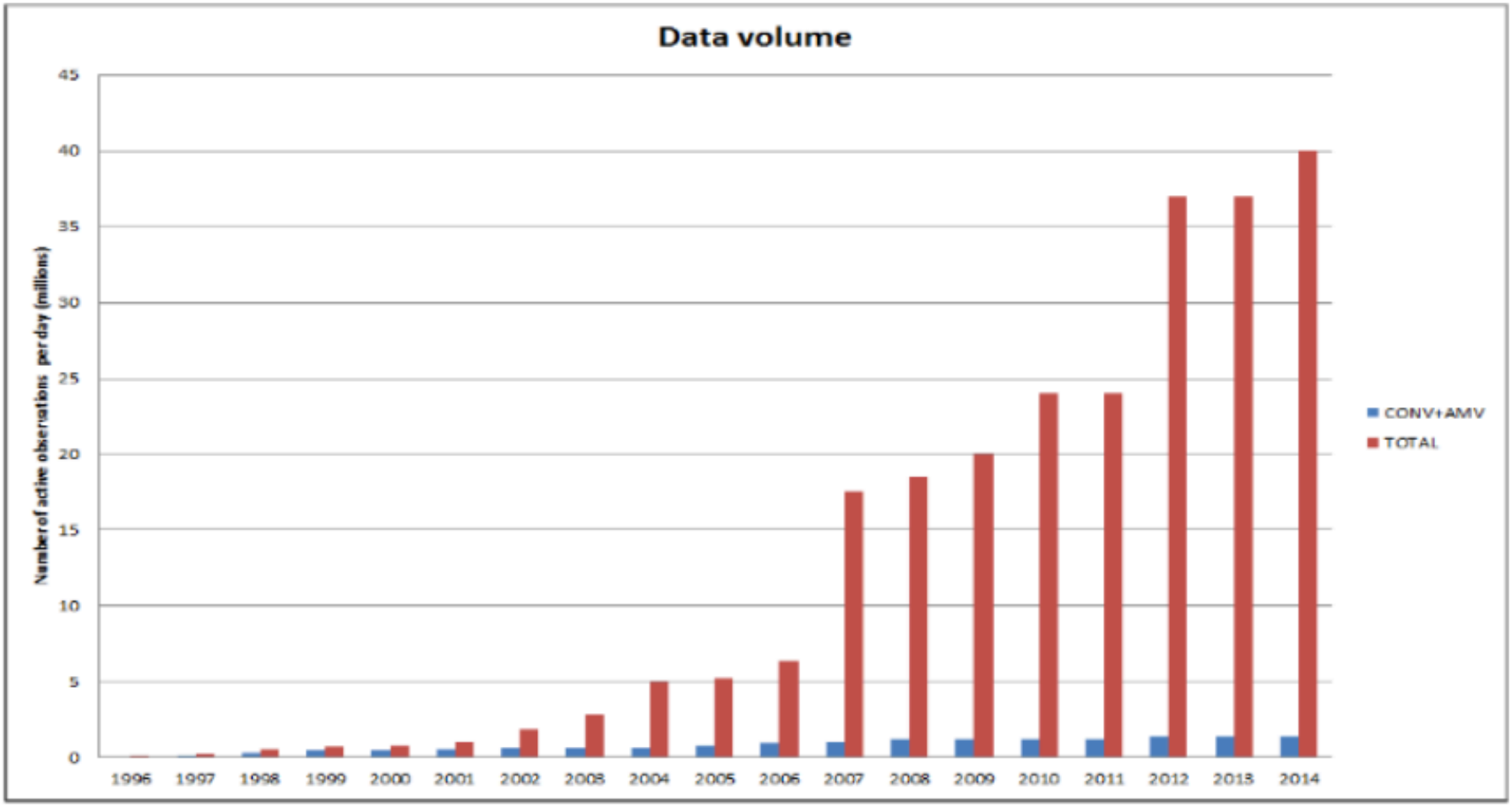
Data volume
Number of active observations per day (millions)
45
40
35
30
25
20
15
10
5
0
1996
1997
1998
1999
2000
2001
2002
2003
2004
2005
2006
2007
2008
2009
2010
2011
2012
2013
2014
CONV+AMV
TOTAL

Satellite *ADM-Aeolus*, put in orbit August 22, 2018, will make Doppler lidar measurements of wind. This is expected to bring significant additional information to present satellite measurements, which bear mostly on the distribution of mass.

- *Synoptic* observations (ground observations, radiosonde observations), performed simultaneously, by international agreement, in all meteorological stations around the world (00:00, 06:00, 12:00, 18:00 UTC)

- *Asynoptic* observations (satellites, aircraft), performed more or less continuously in time.

- *Direct* observations (temperature, pressure, horizontal components of the wind, moisture), which are local and bear on the variables used for for describing the flow in numerical models.

- *Indirect* observations (radiometric observations, …), which bear on some more or less complex combination (most often, a one-dimensional spatial integral) of variables used for for describing the flow

$$y = H(\boldsymbol{x})$$

H : *observation operator (*for instance, radiative transfer equation)

ECMWF data coverage (all observations) - SEA LEVEL ANOMALY

20190216 00

Total number of obs = 5679

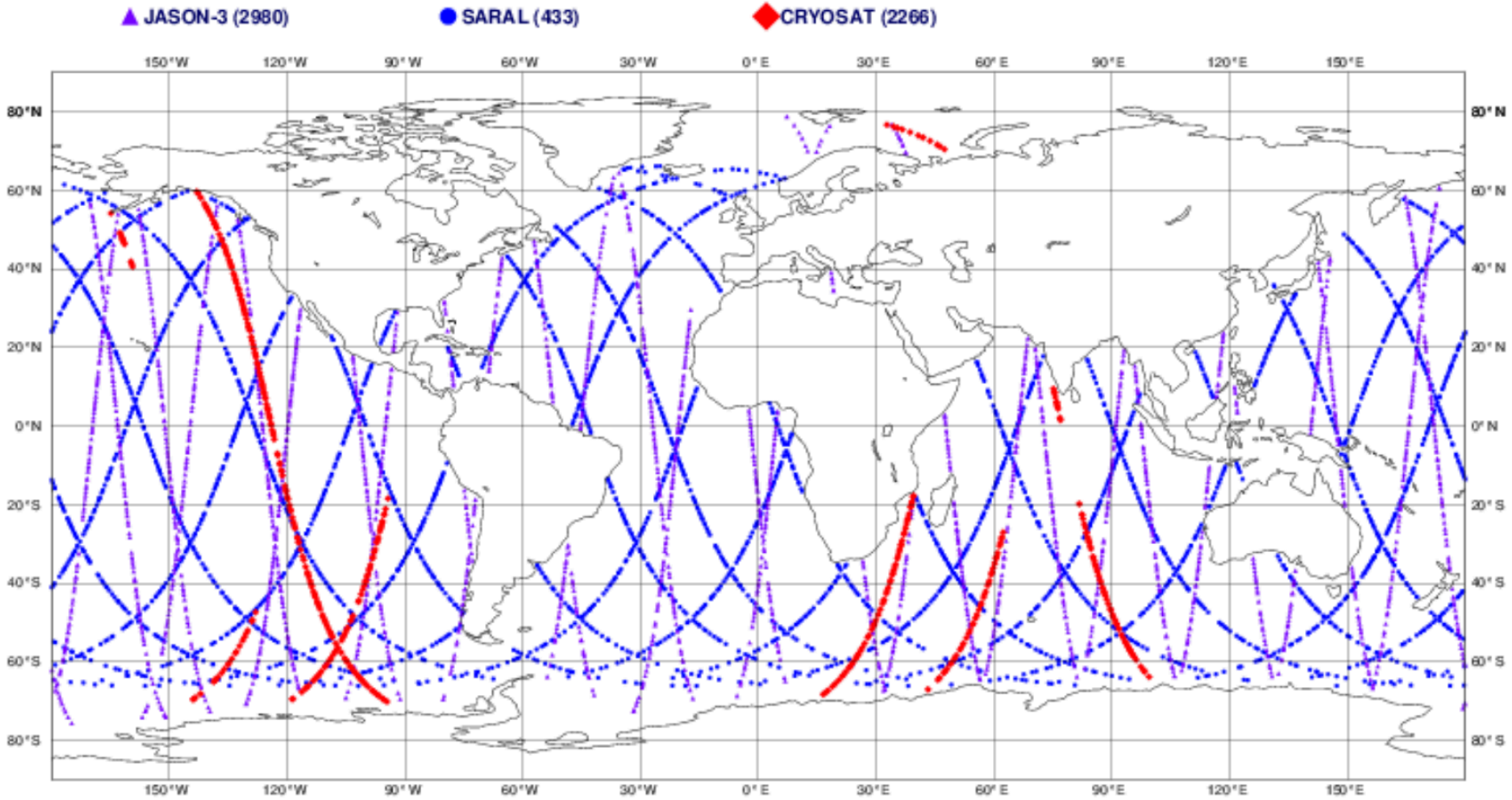

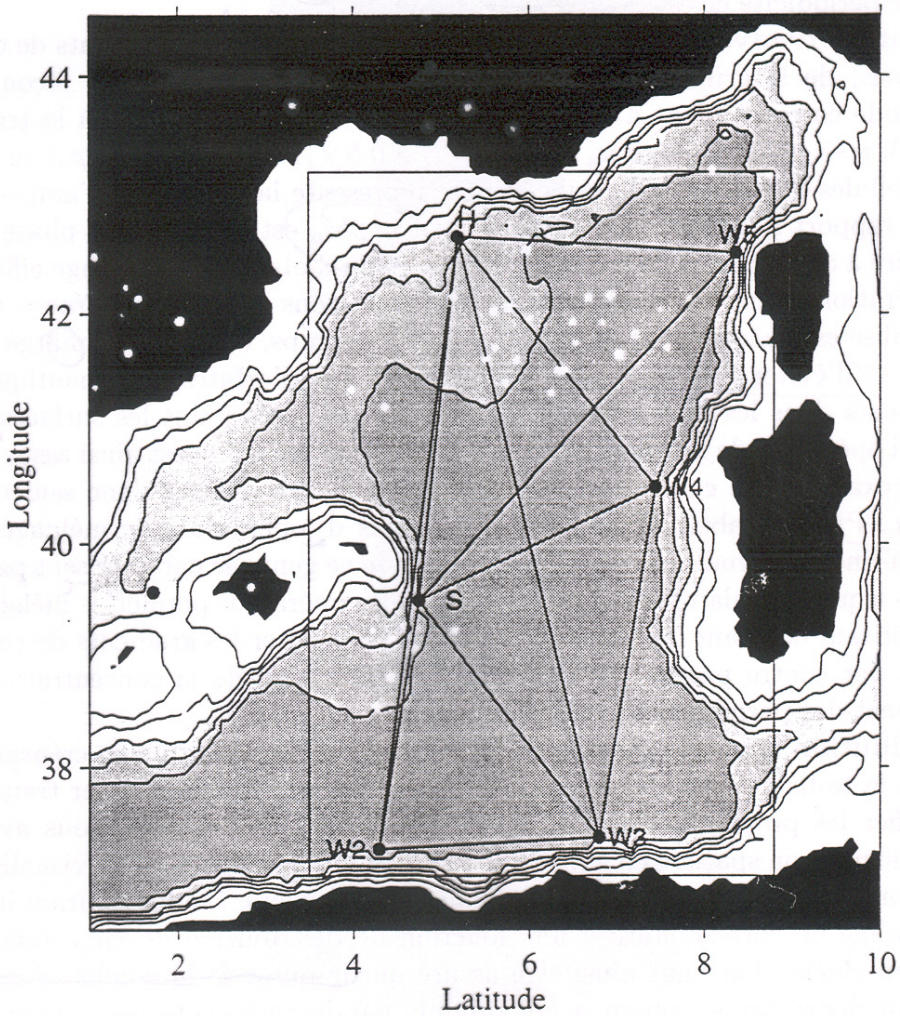

FIG. 1 – *Bassin méditerranéen occidental: réseau d'observation tomographique de l'expérience Thétis 2 et limites du domaine spatial utilisé pour les expériences numériques d'assimilation.*

E. Rémy, Doctoral Dissertation, 1999

Purpose of assimilation : reconstruct as accurately as possible the state of the atmospheric or oceanic flow, using all available appropriate information. The latter essentially consists of

- The observations proper, which vary in nature, resolution and accuracy, and are distributed more or less regularly in space and time.

- The physical laws governing the evolution of the flow, available in practice in the form of a discretized, and necessarily approximate, numerical model.

- 'Asymptotic' properties of the flow, such as, *e. g.*, geostrophic balance of middle latitudes. Although they basically are necessary consequences of the physical laws which govern the flow, these properties can usefully be explicitly introduced in the assimilation process.

Assimilation is one of many '*inverse problems*' encountered in many fields of science and technology

- solid Earth geophysics
- plasma physics
- 'nondestructive' probing
- navigation (spacecraft, aircraft, ….)
- …

Solution most often (if not always) based on Bayesian, or probabilistic, estimation. 'Equations' are fundamentally the same.

Difficulties specific to assimilation of meteorological observations :

- Very large numerical dimensions ($n \approx 10^6$-10^9 parameters to be estimated, $p \approx 4$-5.10^7 observations per 24-hour period). Difficulty aggravated in Numerical Weather Prediction by the need for the forecast to be ready in time.

- Non-trivial, actually chaotic, underlying dynamics

Cours à venir

~~Jeudi 14 Février~~

~~Jeudi 21 Février (**)~~

Jeudi 28 Février

Jeudi 7 Mars

Vendredi 15 Mars

Jeudi 21 Mars (**)

Jeudi 28 Mars (*)

De 10h00 à 12h30, Département de Géosciences, École Normale Supérieure, 24, rue Lhomond, Paris 5, Salle de la Serre, 5ième étage,

(*) Salle E314, 3ième étage

(**) Salle E350, 3ième étage